SCIENTIFIC JOURNAL OF POLISH NAVAL ACADEMY
ZESZYTY NAUKOWE AKADEMII MARYNARKI WOJENNEJ

2018 (LIX) 4 (215)

sciendo

DOI: 10.2478/sjpna-2018-0025

DESIGN PROCESS OF A HELICAL FLUX COMPRESSION GENERATOR

Mariusz Makowski, Marta Czarnowska, Karol Biernacki, Rafał Namiotko

Maritime Technology Center S.A., Arenda Dickmana 62 Str., 81-109 Gdynia, Poland; e-mail: {mariusz.makowski; marta.czarnowska; karol.biernacki; rafal.namiotko}@ctm.gdynia.pl

ABSTRACT

The article demonstrates the design process of a flux compression generator. Several armature configurations and materials have been analyzed. The influence of mechanical parameters, such as wall thickness, inner diameter of the armature or high explosive material used, on FCG performance has been estimated. The geometry of generators' components has been optimized using the Finite Elements Method. Several generators have been built based on mathematical model and simulation results. The designed FCG's performance has been verified during field tests. A comparison of simulation and field test results has been presented.

Key words:
helical flux compression generator design, gurney speed, gurney angle.

Research article

INTRODUCTION

Flux compression generators (FCGs) operate on the principle of forcing initial magnetic flux into progressively degrading inductance in such a way that flux loss is minimized. This is achieved by using explosives to short-out turns in the field coil (stator) via a conductive expanding tubing (armature) [1, 3].

The expanding armature forms a cone travelling at a certain speed called the Gurney's speed [8]. The Gurney speed is expressed by eq. (1).

$$V_G = \sqrt{2E}\left(\frac{M}{C}+\frac{n}{n+2}\right)^{-\frac{1}{2}} = \sqrt{2E}\left(\frac{M}{C}+\frac{1}{2}\right)^{-\frac{1}{2}}, \tag{1}$$

where:

n — geometry defining parameter — for cylindrical samples n = 2;

M — armature mass;

C — explosive charge mass;

$\sqrt{2E}$ — Gurney constant.

In order to achieve the highest current amplification it is paramount to maximize the Gurney speed of the armature. The speed, as can be seen in (eq. 1), is affected by the ratio of explosive charge mass to the armature mass [8].

During the FCG design phase it is critical to keep a balance between a low armature mass and its ability to expand without fracturing in order to keep the Gurney speed at the highest possible level.

SIMULATIONS

The design of mechanical parts of an FCG has been based on finite elements analysis using the ANSYS Autodyn software. Mathematical and physical model was based on equations of state (EOS) available in software. EOS JWL (Jones, Wilkins, Lee) was used for explosive materials and EOS Shock for other materials. The simulations are a good method to optimize the size, geometry, placement and material of certain parts of an FCG. A cross-section of a helical FCG model has been presented in fig. 1.

The presented model was used to ascertain the behavior of support elements, and conductor insulation. It was also helpful in determining the proper shape of the crowbar and the maximum expansion ratio of the armature before it started to develop fractures.

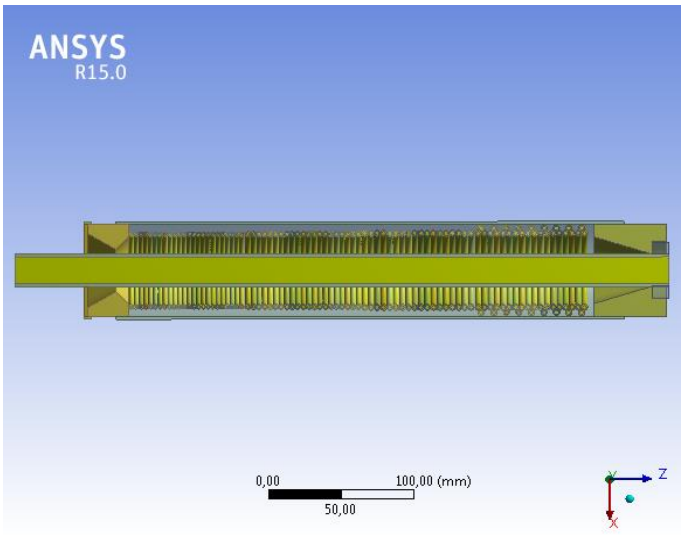

Fig. 1. FCG model cross-section

The Gurney speed and angle have been estimated by placing control points along the armature axis as presented in fig. 2.

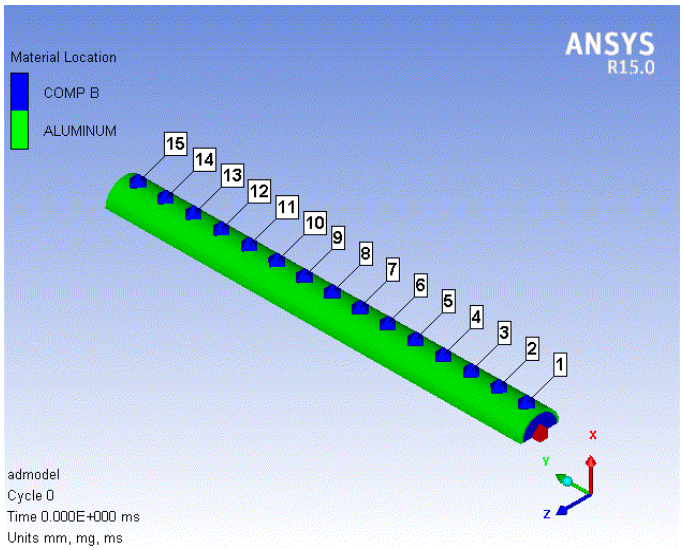

Fig. 2. Control points placed along the axis of the armature

This design phase has been divided into two sections — parametric analysis and strength of materials.

Parametric analysis

The first step was determining the high explosive material to be used in the designed model. The choice criterions were the availability, low sensitivity, ease of uniform elaboration and velocity of detonation. Two chosen materials were TNT and Composition B placed in aluminum armatures. The two explosive materials of equal mass have been compared for the highest obtainable Gurney angle and speed as presented in tab. 1 and fig. 3.

Tab. 1. Explosive materials comparison

Explosive material	**Composition B**	**TNT**
Armature inner diameter [mm]	23	23.6
Armature outer diameter [mm]	27	27.6
Armature length [mm]	350	350
Mass of explosive material [g]	249.7	249.6
Gurney speed [km/s]	**2.6**	**2.2**
Gurney angle [deg]	**18.31**	**16.98**

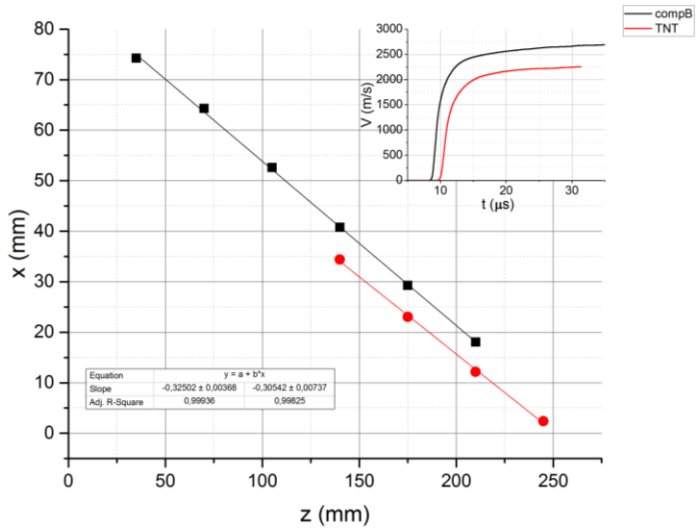

Fig. 3. Gurney speed and armature wall deformation for TNT (red) and composition B (black); armature wall deformation at 37.5 μs (TNT) and 35 μs (composition B) after detonation initiation; steeper angle equals higher velocity of detonation

A slightly greater diameter of TNT-based armature has been chosen in order to maintain equal mass of both explosive materials due to a slight difference of their density. Composition B appears to be a better choice due to a slightly higher Gurney

speed (approx. 18% higher), however the elaboration is not homogenous due to RDX insolubility in TNT and has to be taken into account during the design phase. The detonation velocity sharply rises in the first stage, due to the influence of the detonation wave front, to achieve a maximum value according to Gurney's model [5, 9].

Next comparison was of the armature material. Two obvious choices of copper and aluminum armatures of same dimensions are presented in tab. 2 and fig. 4. The simulation results show that aluminum seems to be the better choice due to its lower mass, however its ductility is much lower than copper's which contributes to a lower expansion ratio due to longitudinal cracking. This will be further discussed in the following sections.

Tab. 2. Armature material comparison

Armature material	**Aluminum**	**Copper**
Armature inner diameter [mm]	25	25
Armature outer diameter [mm]	28	28
Armature length [mm]	300	300
Armature mass [g]	101.36	333.22
Mass of explosive material [g]	252.85	252.85
Gurney speed [km/s]	**2.92**	**1.98**
Gurney angle [deg]	**18.56**	**13.09**

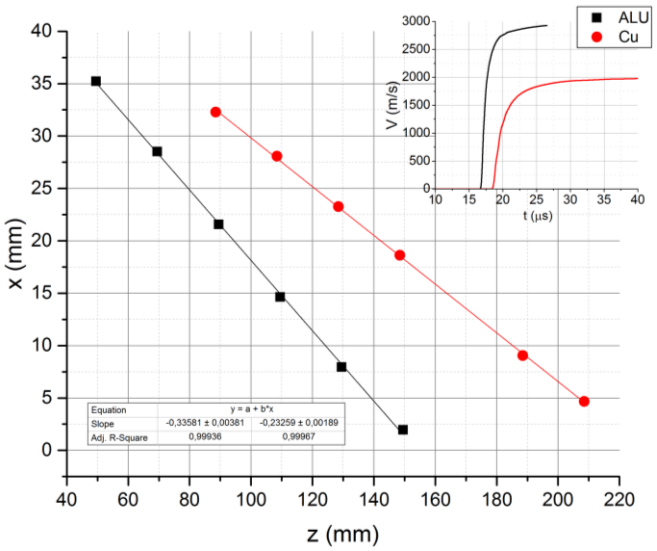

Fig. 4. Gurney speed and armature wall deformation for copper (red) and aluminum (black); armature wall deformation at 20 µs (aluminum) and 30 µs (copper) after detonation initiation; steeper angle equals higher velocity of detonation

Another comparison stage was performed for the assessment of armature length influence on Gurney speed and angle. Simulation was performed for aluminum armatures of equal diameter and wall thickness. The results were uniform as expected and are shown in tab. 3 and fig. 5. If the explosive material used is homogenous and the elaboration is uniform then the velocity of detonation (and consequently Gurney speed) reaches a maximum and remains constant independently of the length of the armature.

Tab. 3. Armature length comparison

Armature length [mm]	**100**	**300**
Armature inner diameter [mm]	15	15
Armature outer diameter [mm]	17	17
Armature mass [g]	13.6	40.8
Mass of explosive material [g]	30.3	91
Gurney speed [km/s]	**2.77**	**2.81**
Gurney angle [deg]	**18.42**	**18.38**

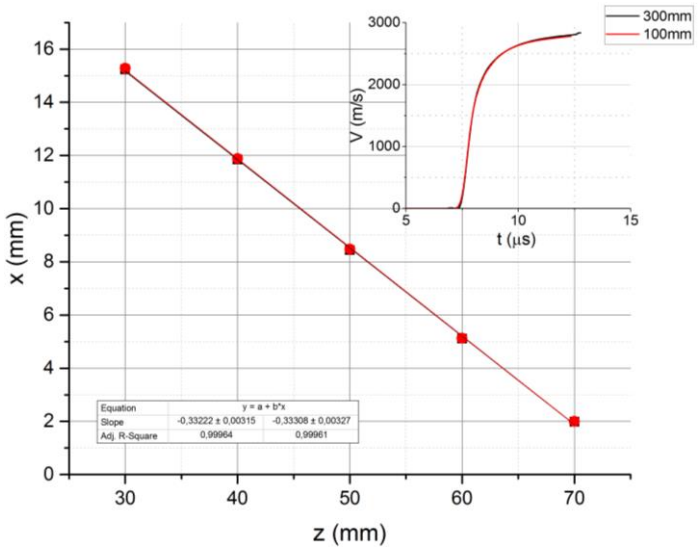

Fig. 5. Gurney speed and armature wall deformation for armature length of 100 mm (red) and 300 mm (black) at 10 μs after detonation initiation; steeper angle equals higher velocity of detonation

The influence of wall thickness has also been ascertained. The analysis was performed for aluminum armatures of same dimensions and equal mass of explosive material. Wall thickness defined the outer diameter of armatures as described in tab. 4.

Tab. 4. Armature wall thickness comparison

Armature wall thickness [mm]	**1**	**2**	**4**
Armature inner diameter [mm]	15	15	15
Armature outer diameter [mm]	17	19	23
Armature length [mm]	100	100	100
Armature mass [g]	13.6	28.9	64.6
Mass of explosive material [g]	30.3	30.3	30.3
Gurney speed [km/s]	**2.77**	**2.2**	**1.51**
Gurney angle [deg]	**18.42**	**14.55**	**9.27**

The best results (highest Gurney speed and angle) were obtained for the smallest wall thickness however, as has been pointed out in previous section, a small thickness is not always practical (for large diameter stators) as it develops longitudinal cracks during expansion much sooner. Increasing the wall thickness over a certain point also produces negative results as speed oscillations begin to appear due to pressure equalization between the inner and outer surface of an expanding armature wall [9] as can be seen in fig. 6.

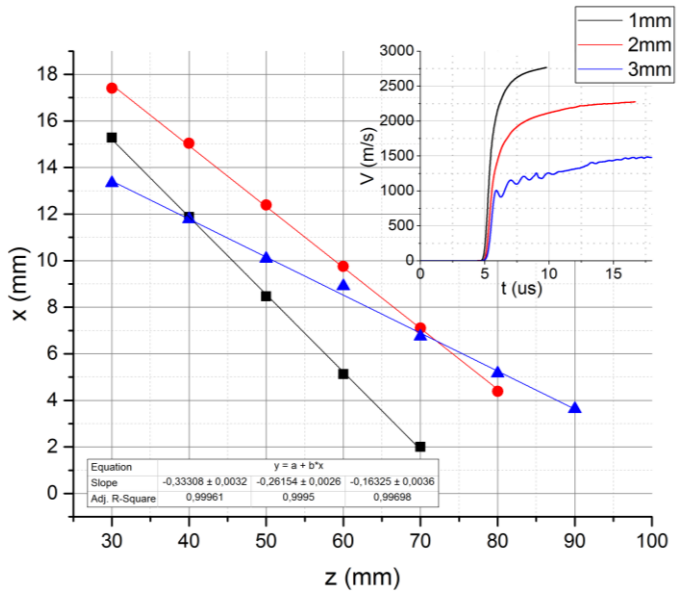

Fig. 6. Gurney speed and armature wall deformation for armature wall thickness of 1 mm (black), 2 mm (red) and 3 mm (blue); armature wall deformation at 10 μs (1 mm), 13 μs (2 mm) and 15 μs (3mm) after detonation initiation; steeper angle equals higher velocity of detonation

Component material strength analysis

Armature

During the design phase of FCG components the dimensions and materials must be carefully chosen. For instance the ductility of armature material needs to be as high as possible and the wall thickness has to be chosen accordingly so as not to allow the formation of longitudinal cracks before the expanding cone reaches the stator winding. On the other hand increasing the wall thickness lowers the Gurney speed and angle which contribute to lower current amplification and to possible formation of electrical arcs in front of the progressing cone [1, 8].

Another aspect to consider is the material resistance to shock-wave loading. The armature may fracture due to the explosive shock-wave and wall thickness has to be determined so as to provide proper mechanical strength. The simulations were performed for an aluminum armature of equal inner diameter and length and a wall thickness of 4 mm and 5 mm.

Each simulation model is built using ideal materials, so the results need to be confronted with real-life possibilities of internal defects and proper margin of error has to be included. During the design of a model for field tests the wall thickness was set approximately 25% greater than the simulated optimum. In order to improve the ductility of the armature material and remove any internal stress a heat-treatment was applied to the tubes [8].

The conical deformation of the armature in not a uniform process especially at the edges where the detonation front is more oval as shown in fig. 8 and 9. This imposes the need to provide extra length for the armature to develop a cone before it starts to short-out the stator winding. Each FCG geometry has to be evaluated independently to ensure a controlled armature expansion. The shockwave front may also be shaped by some form of explosive lenses but that is outside of the scope of this article.

The time-dependent deformation of different wall thickness armatures is shown in fig. 7 and 9. It can be seen that the material develops cracks at different distances from the axis so, again, a certain margin of error needs to be imposed during the design process. The phenomenon is further demonstrated in fig. 8 where the longitudinal cracking is visible as ripples on the surface of the armature.

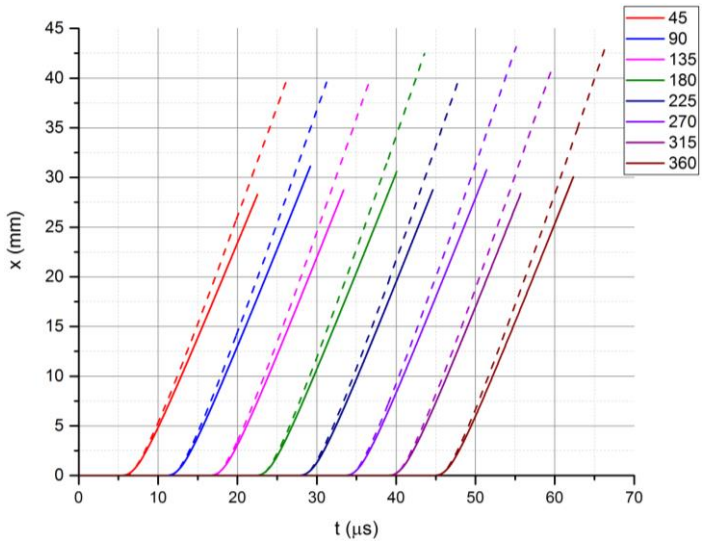

Fig. 7. Time-dependent armature deformation for a wall thickness of 4 mm (full line) and 5 mm (dashed line) for control points spaced 45 mm apart

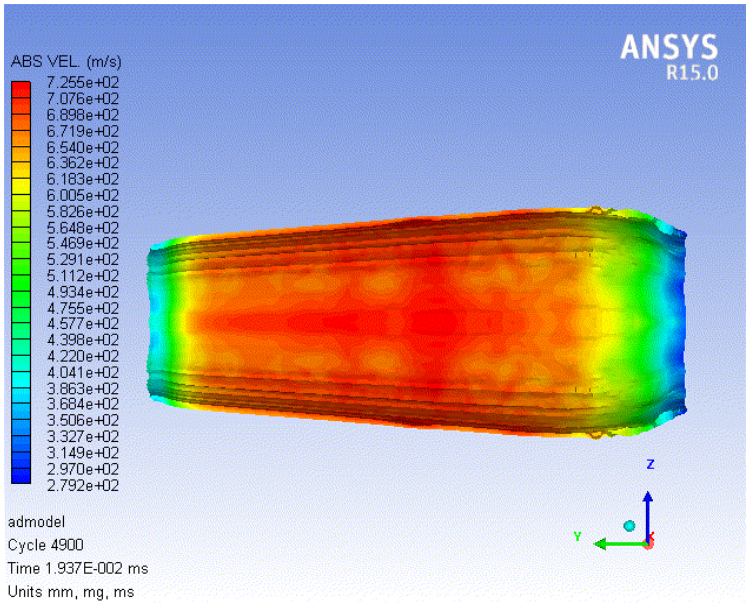

Fig. 8. Uneven surface deformation and oval-shaped deformation at the edges of the armature

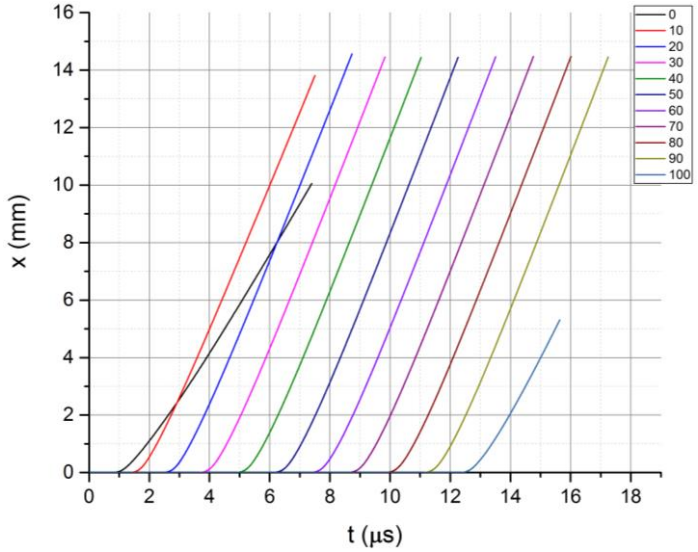

Fig. 9. Time-dependent armature deformation with lower Gurney speed at the edges of the armature

Stator winding insulation

The electrical insulation of stator winding is a critical parameter to evaluate. It needs to provide proper dynamic voltage insulation and at the same time not interfere with quick shorting of the turns by the travelling cone. A simplified simulation model was used in the evaluation process of different kinds of wire insulations as presented in fig. 10.

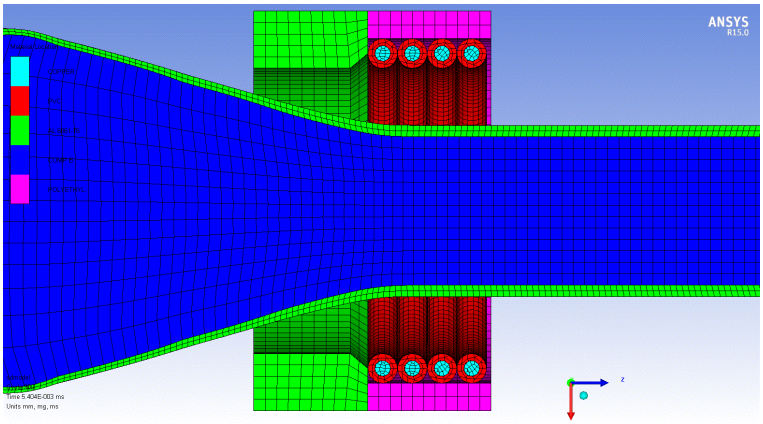

Fig. 10. A simplified simulation model for the analysis of wire insulation under dynamic loading

Stator-armature alignment and crowbar

Additional elements such as crowbar and alignment rings need to be carefully designed as well. Proper alignment of stator and armature is one of the most important factors to consider during the design and construction of a successful FCG. Even the slightest misalignment on the order of a few per cent results in a complete failure to compress flux and amplify current. Furthermore the aligning elements cannot damage or interfere with the expansion of the armature.

The crowbar performs the unique function of shorting-out of the seed-current source and beginning of the flux compression process. It needs to maintain good contact with the stator when the expanding armature hits it and must not damage the armature upon impact so as to maintain a proper electrical connection. It also needs to allow for a smooth and quick shorting-out of the source without any electrical arcing forming to avoid any loss of energy at the beginning of flux compression.

Several geometries have been analyzed, as shown in fig. 11 and 12, considering the work of other authors [2]. It has been observed that every FCG geometry requires an individually designed crowbar for proper operation.

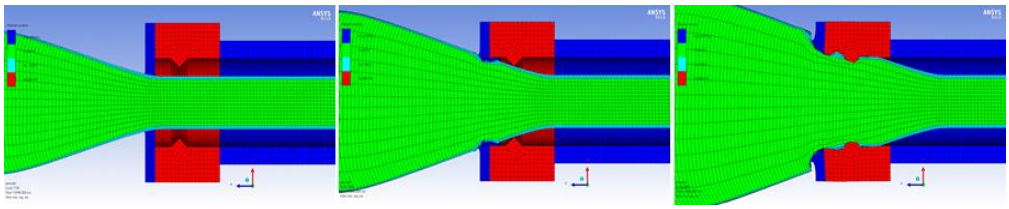

Fig. 11. Performance analysis of aligning rings and crowbar during armature expansion

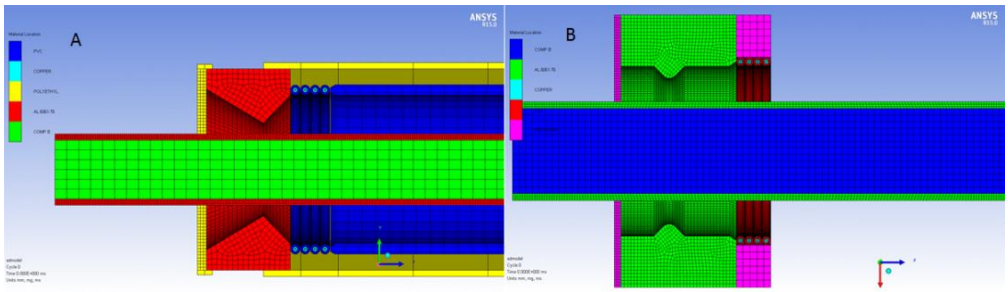

Fig. 12. Different crowbar geometries

Simulations summary

Presented simulation results point out certain key aspects of the design process of a FCG. It has been shown that the proper choice of explosive material and the ratio of explosive to armature mass have a huge impact on the potential flux compression capability of the designed generator. The choice of armature material and wall thickness is a difficult compromise between mechanical strength and FCG performance. Every component needs to be carefully evaluated when constructing a successful flux compression generator.

FIELD TESTS

Several field tests have been performed in order to verify the simulation results. Although the verification of certain qualities of a designed FCG requires a sophisticated lab setup with a fast x-ray camera, a streak-shutter camera etc., the measurement of velocity of detonation of used High Explosive and the generated current provide enough data to assess whether a given FCG is a successful one.

The FCG under tests was developed based on a mathematical model in conjunction with simulations using the ANSYS Autodyn software.

Simulation vs. field tests

Velocity of detonation of a composition B charge has been measured in two different setups as in fig. 15 in order to minimize readout errors. The velocity measured at 7.98 km/s and is in good agreement with theoretical data [5]. The simulation results also confirm the measured velocity of detonation. The velocity of detonation in ANSYS software was measured indirectly by observing the pressure change in control points generated by the travelling shockwave as presented in fig. 13 and 14. The results of field tests are shown in tab. 5 and fig. 16.

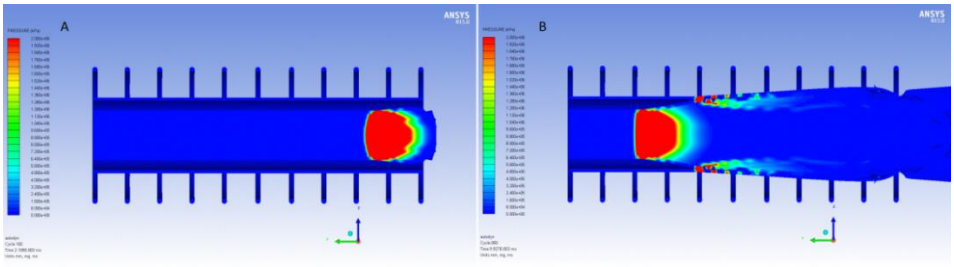

Fig. 13. Detonation wave front at A) 2 μs and B) 10 μs after detonation initiation

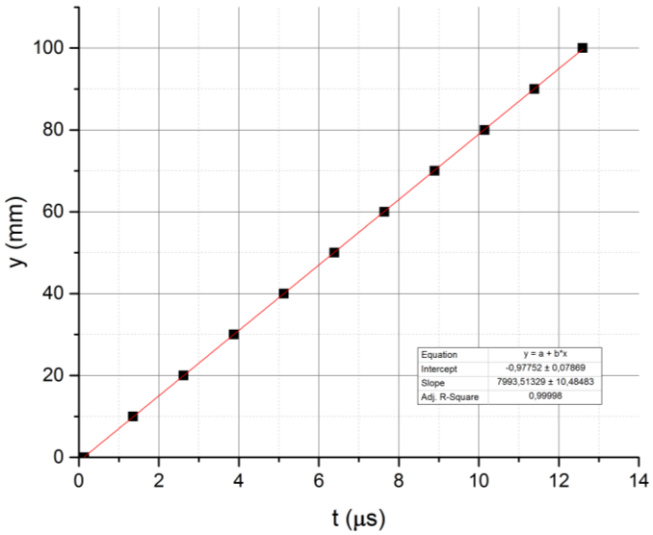

Fig. 14. Time-dependent detonation wave front position

Fig. 15. Field test setups for velocity of detonation measurement

Measurement uncertainties in the simulation software are caused by the mesh size and are considered insignificant. For simulation purpose the composition B mixture consisting of 64% RDX and 36% TNT by weight was chosen, while the mixture used during field test was measured to consist of 60–70% RDX and 40–30% TNT by weight. Also the copper tube seems to be a little faster — this might be caused by a part of aluminum tubing reacting with the explosive material.

Tab. 5. Simulated and measured velocity of detonation comparison

	V_d [km/s]	dV_d [km/s]
Experiment 1 (aluminum tube)	7.786	0.062
Experiment 2 (copper tube)	7.848	0.149
Simulation	7.99	0.02

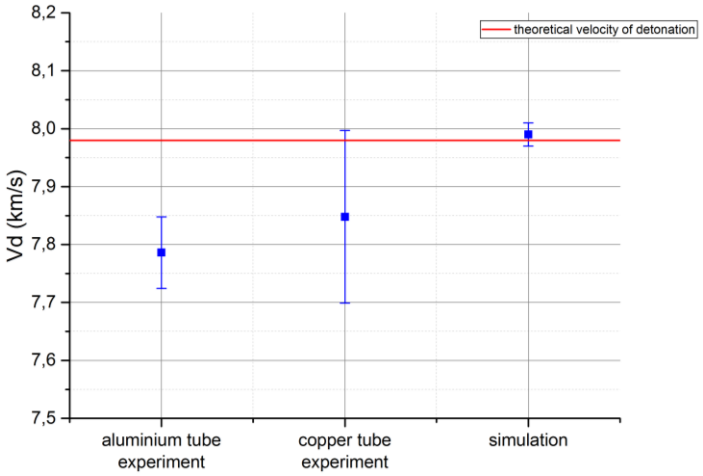

Fig. 16. Velocity of detonation comparison;
from left to right: aluminum tube, copper tube, simulation

FCG design example and field tests

Several models of flux compression generators have been designed by our team based on a mathematical model and simulations in ANSYS Autodyn software. An example of a designed FCG is presented in fig. 17 and 18.

The armature was made with aluminum 6060 tube with inner diameter of 19 mm, outer diameter of 22 mm and a length of 450 mm. The stator winding inner diameter was 48 mm and divided into sections of variable pitch, wire cross-section and parallel wire number to minimize flux losses. The generator was loaded with a single-turn coil of a flat bus-bar with approx. 400 nH inductance. Current measurements are presented in fig. 19.

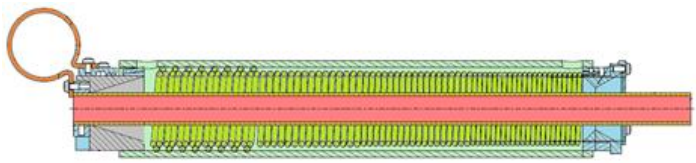

Fig. 17. Designed FCG cross-section

Fig. 18. Design FCG during field tests

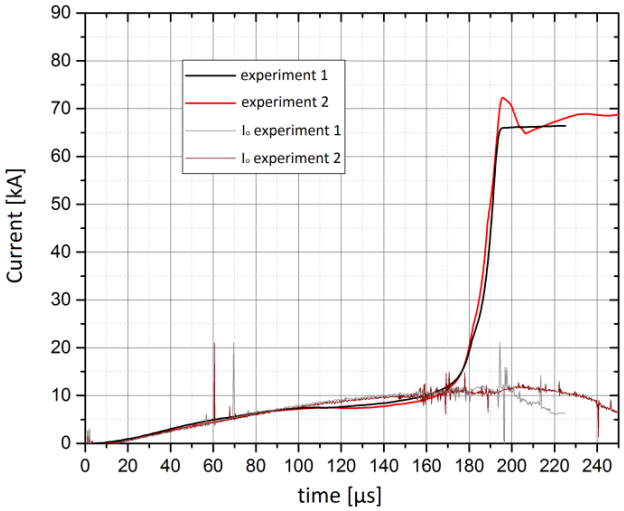

Fig. 19. Two trials of a designed FCG geometry: grey and brown lines — seed current for trial run No. 2 and 3 respectively, black and red lines — output current for trial runs No. 2 and 3 respectively

The seed current was 10 kA, FCG time of about 50 μs starts at 160 μs and ends at 210 μs. Trial run No. 2 has not been fully registered due to the exceeding of oscilloscope range. It can be seen that an amplification factor of at least 7 has been achieved with the output current in the range of 70 kA. While the value itself is not the highest obtainable, the model was designed as a proof of concept of the validity of the mathematical model aided by explosive simulations in the ANSYS Autodyn software.

CONCLUSIONS

Simulations performed with the use of finite elements analysis offer a large range of possibilities to accurately design the components of a flux compression generator. The simulations in conjunction with a strong mathematical model form a complete design tool to build a functional FCG while taking into consideration all the challenges posed by the proper choice of material and geometry of the components.

The field tests performed by our team confirm the validity of simulations using the ANSYS Autodyn software for the design of a successful flux compression generator.

Acknowledgements

This work was supported by National Centre for Research and Development in Poland (Grant No. DOB-1-1/1/PS/2014).

REFERENCES

[1] Altgilbers L. L., Brown M. D. J., Grishnaev I., Novac B. M., Smith I. R., Tkach I., Tkach Y., *Magnetocumulative Generators*, Series Shock Wave and High Pressure Phenomena, Springer-Verlag New York, 2000.

[2] Appelgren P., *Experiments with and modelling of explosively driven magnetic flux compression generators*, KTH School of Electrical Engineering, Space and Plasma Physics, Royal Institute of Technology, Stockholm 2008.

[3] Appelgren P., Bjarnholt G., Brenning N., Elfsberg M., Hurtig T., Larsson A., Novac B. M., Nyholm S. E., *Small Helical Magnetic Flux-Compression Generators: Experiments and Analysis*, 'IEEE Transactions on Plasma Science', 2008, Vol. 36, No. 5, pp. 2662–2672.

[4] Bola M. S., Madan A. K., Singh M., Vasudeva S. K., *Expansion of Metallic Cylinders under Explosive Loading*, 'Defence Science Journal', 1992, Vol. 42, No. 3, pp. 157–163.

[5] Dobratz B. M., Crawford P. C., *Explosives handbook — properties of chemical explosives and explosives simulants*, January 1985.

[6] Elek P., Jaramaz S., Micković D., *Modeling of the metal cylinder acceleration under explosive loading*, 'Scientific Technical Review', 2013, Vol. 63, No. 2, pp. 39–46.

[7] Hutchinson M. D., *With-Fracture Gurney Model to Estimate both Fragment and Blast Impulses*, 'Central European Journal of Energetic Materials', 2010, Vol. 7, No. 2, pp. 175–186.

[8] Neuber A. A., *Explosively Driven Pulsed Power Helical Magnetic Flux Compression Generators*, Springer-Verlag Berlin Heidelberg, Series Power Systems, 2005.

[9] Scott I. J., *Scaled Cylinder Test Experiments with Insensitive PBX 9502 Explosive*, 15th International Detonation Symposium, San Francisco — California 2014.

MODELOWANIE I BUDOWA SPIRALNEGO GENERATORA MAGNETOKUMULACYJNEGO

STRESZCZENIE

W artykule scharakteryzowano proces projektowania elementów generatora magnetokumulacyjnego. Przeprowadzono analizę porównawczą kilku konfiguracji i materiałów tworników FCG. Oszacowano wpływ na działanie generatora parametrów mechanicznych, takich jak materiał rurki, grubość ścianki, średnica wewnętrzna rurki, rodzaj materiału wybuchowego. Dokonano optymalizacji geometrii podzespołów generatora za pomocą metody elementów skończonych. W oparciu o model matematyczny i symulacje wykonano modele i przeprowadzono próby poligonowe z ich wykorzystaniem. Porównano wyniki symulacji z wynikami badań poligonowych modeli generatorów magnetokumulacyjnych spiralnych.

Słowa kluczowe:

spiralny generator magnetokumulacyjny, prędkość Gurneya, kąt Gurneya.

Article history

Received: 28.05.2018
Reviewed: 04.12.2018
Revised: 07.12.2018
Accepted: 10.12.2018